2014
International Symposium on Power Electronics,
Electrical Drives, Automation and Motion

Control of a Power Supply with Cycling Current Using Different Controllers

António Roque and José Maia
Department of Electrical Engineering
ESTSetúbal - Instituto Politécnico de Setúbal & INESC-ID
Setúbal, Portugal
antonio.roque@estsetubal.ips.pt, jose.maia@estsetubal.ips.pt

Elmano Margato
Centro de Electrotecnia e Electrónica Industrial
ISEL &INESC-ID
Lisboa, Portugal
efmargato@isel.ipl.pt

Duarte M. Sousa and Gil Marques
Department of Electrical and Computer Engineering
Instituto Superior Técnico & INESC-ID – Universidade de Lisboa
Lisboa, Portugal
duarte.sousa@tecnico.ulisboa.pt, gil.marques@tecnico.ulisboa.pt

***Abstract*—Fast Field Cycling (FFC) Nuclear Magnetic Resonance (NMR) relaxometers require controlled current sources in order to get accurate flux density with respect to its magnet. The main elements of the proposed solution are a power semiconductor, a DC voltage source and the magnet. The power semiconductor is commanded in order to get a linear control of the flux density. To implement the flux density control, a Hall Effect sensor is used. Furthermore, the dynamic behavior of the current source is analyzed and compared when using a PI controller and a PD2I controller.**

Keywords*— *power supply, flux density; current; control; Fast Field Cycling NMR; relaxometer

I. Introduction

The flux density of a Fast Field Cycling (FFC) Nuclear Magnetic Resonance (NMR) is directly related with the current demanded by the used magnet [1-4]. As typical requirements, the flux density should cycle as shown in Fig. 1 with a ratio of about 0.1 T/ms [5-9]. In addition, from cycle to cycle, the low level of the flux density can be adjusted and the flux density levels should be defined with accuracy.

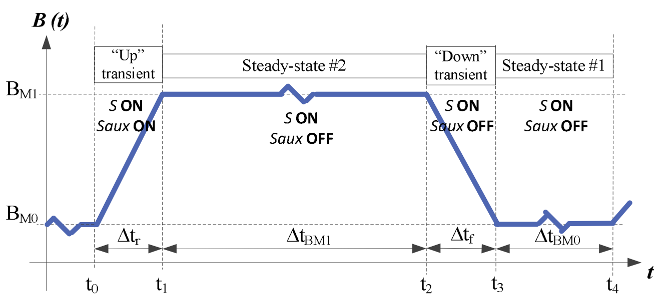

Fig. 1. Flux density cycle of a FFC NMR relaxometer.

In this paper, the dynamic behavior and flux density control of the FFC NMR power supply in Fig. 2 is analyzed when testing controllers with two different configurations (PI and PD2I).

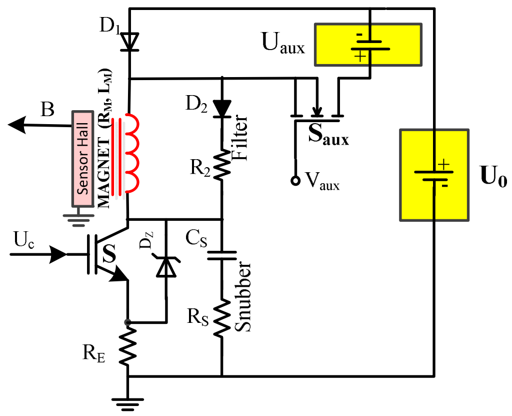

Fig. 2. Electric circuit of the power supply.

II. Control

The operating modes of the proposed topology are the following [10]:

- *Up*: fast flux density transition from a low level (B_{M0}) to a high level (B_{M1});
- *Steady-state #1*: steady-state flux density when the flux density is at the high level, corresponding to the "polarization" level or the "detection level" of a FFC NMR experiment;
- *Down*: fast flux density transition from a high level (B_{M1}) to a low level (B_{M0});
- *Steady-state #2*: steady-state flux density when the flux density is at a low level, corresponding to the "evolution" level of a FFC NMR experiment; this flux density level is adjusted from cycle to cycle, according to the experimental requirements.

978-1-4799-4749-2/14/$31.00 ©2014 IEEE

In Fig. 3, the circuit with a closed loop control system is shown.

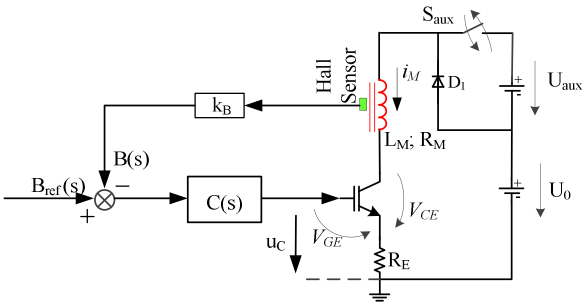

Fig. 3. Diagram of the circuit with the control system.

In order to understand the running of the proposed solution it is important to refer that: the auxiliary power source U_{aux} is only connected during the "Up" transient in order to accelerate the flux density transition [10]; and, commanding the semiconductor S, the magnet current i_M can be set adjusting the collector-emitter voltage V_{CE}.

The gain K_B of the Hall Effect circuit depends mainly on the characteristics of the magnet (B=f(i_M)). Considering the available magnet [10], K_B=0.04V/T.

Under these conditions, it is assumed a linear relationship between V_{CE} and the gate-emitter voltage V_{GE}.

$$\frac{\Delta V_{CE}}{\Delta V_{GE}} = -\beta \tag{1}$$

The parameter β=700 is considered based on the characteristics of the semiconductor used and the minimum value of V_{CE} that assures safe operation of the IGBT [10].

According to the Fig. 3 circuit, V_{GE} depends on the command voltage U_C and on the emitter resistance R_E.

$$\Delta V_{GE} = \Delta u_c - R_E \Delta i_M \tag{2}$$

So that and according to the typical specifications of the FFC NMR apparatus, the flux density should be dynamically controlled considering either a step or a ramp as reference inputs. Under these conditions, two controllers will be tested.

A. PD2I controller

The block diagram for a PD2I controller (proportional, derivative and two integral actions) is represented in Fig. 4.

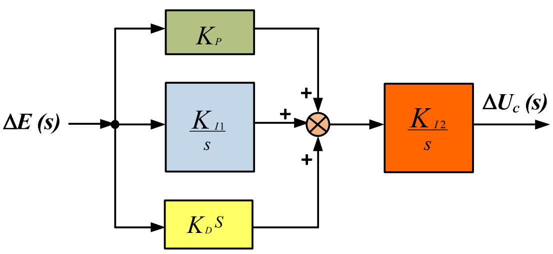

Fig. 4. Block diagram of the PD2I controller.

Being the transfer function of the PI2D controller:

$$\frac{\Delta U_C(s)}{\Delta E(s)} = C(s) = k_D k_{I2} \frac{s^2 + \frac{k_P}{k_D}s + \frac{k_{I1}}{k_D}}{s^2} \tag{3}$$

The global block diagram of the proposed circuit can be simplified as shown in Fig. 5.

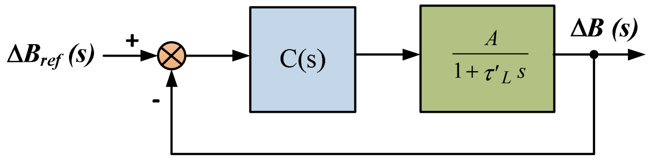

Fig. 5. Block diagram of the proposed circuit with the controller.

The global transfer function is:

$$\frac{\Delta B(s)}{\Delta B_{ref}(s)} = \frac{k_D k_{I2} A}{\tau'_L} \frac{s^2 + \frac{k_P}{k_D}s + \frac{k_{I1}}{k_D}}{s^3 + \frac{1+K_D K_{I2} A}{\tau'_L}s^2 + \frac{K_P K_{I2} A}{\tau'_L}s + \frac{K_{I1} K_{I2} A}{\tau'_L}} \tag{4}$$

Being:

$$A = \frac{\beta \cdot k_B}{(R_t + \beta R_E)} \approx \frac{k_B}{R_E} \tag{5}$$

$$\tau'_L = \frac{R_t}{(R_t + \beta R_E)} \tau_L \approx \frac{R_t}{\beta R_E} \tau_L \tag{6}$$

$$\tau_L = \frac{L_M}{R_M + R_E} = \frac{L_M}{R_t} \tag{7}$$

Where L_M represents the self-inductance of the magnet R_M is the resistance of the magnet and R_E is the emitter resistance.

As first approach, considering K_D=0, the transfer function (4) becomes:

$$\frac{\Delta B(s)}{\Delta B^*(s)} = \frac{\frac{k_P K_{I2} A}{\tau'_L}s + \frac{K_{I1} K_{I2} A}{\tau'_L}}{s^3 + \frac{1}{\tau'_L}s^2 + \frac{k_P K_{I2} A}{\tau'_L}s + \frac{K_{I1} K_{I2} A}{\tau'_L}} \tag{8}$$

For this type of system, the static speed error should be minimized. Using the criteria ITAE, the 3rd order optimized transfer function is given by [11-13]:

$$FT_{opt}(s) = \frac{3{,}25\omega_0^2 s + \omega_0^3}{s^3 + 1{,}75\omega_0 s^2 + 3{,}25\omega_0^2 s + \omega_0^3} \tag{9}$$

Based on this approach, the parameters of the control system should be set according the following conditions:

$$K_{I1} K_{I2} = \frac{1}{(1{,}75)^3 {\tau'_L}^2 A} \tag{10}$$

$$K_P K_{I2} = \frac{3{,}25}{(1{,}75)^2 \tau'_L A} \tag{11}$$

B. PI controller

The typical transfer function of a PI controller (proportional and integral actions) is:

$$C(s) = \frac{\Delta U_C(s)}{\Delta E(s)} = k_P + \frac{k_I}{s} = k\frac{1+\tau_Z s}{s} \tag{12}$$

Using the PI controller, the global closed loop transfer function for the proposed system becomes:

$$\frac{\Delta B(s)}{\Delta B_{ref}(s)} = \frac{\frac{K(1+\tau_Z s)}{s}\frac{A}{(1+\tau'_L s)}}{1+\frac{K(1+\tau_Z s)}{s}\frac{A}{(1+\tau'_L s)}} \tag{13}$$

Assuming that,

$$\tau_Z = \frac{\tau'_L}{n} \text{ and } n > 8 \quad (14)$$

expression (13) can be simplified, being:

$$\frac{\Delta B(s)}{\Delta B_{ref}(s)} \cong \frac{\frac{AK}{\tau'_L}}{s^2 + \frac{1+AK\tau_Z}{\tau'_L}s + \frac{AK}{\tau'_L}} \quad (15)$$

In this case, the optimized transfer function can be represented as:

$$FT_{opt}(s) = \frac{\omega_0^2}{s^2 + \sqrt{2}\omega_0 s + \omega_0^2} \quad (16)$$

Considering (15) and (16), the following equations, under optimized conditions, are obtained:

$$\omega_0^2 = \frac{AK}{\tau'_L} \quad (17)$$

$$\omega_0 = \frac{1+AK\tau_Z}{\sqrt{2}\tau'_L} \quad (18)$$

And joining (17) and (18),

$$\left(\frac{1+AK\tau_Z}{\sqrt{2}\tau'_L}\right)^2 = \frac{AK}{\tau'_L} \quad (19)$$

The polynomial characteristic of the proposed system is therefore:

$$0 = K^2 + \frac{2}{A}\frac{(\tau_Z - \tau'_L)}{\tau_Z^2}\mathrm{K} + \frac{1}{(A\tau_Z)^2} \quad (20)$$

In order to get a stable system, the following condition should be observed:

$$\frac{(\tau_Z - \tau'_L)^2}{\tau_Z^2} - 1 > 0 \quad (21)$$

So those, the parameter $K=K_I$ can assume the following values:

$$K_{1,2} = \frac{n}{A\tau'_L}\left[(\mathrm{n}-1) \pm \sqrt{(1-n)^2 - 1}\right] \quad (22)$$

Or as function of the original parameters:

$$K_{1,2} = \frac{\beta R_E{}^2}{K_B R_t}\frac{n}{\tau_L}\left[(n-1) \pm \sqrt{(1-n)^2 - 1}\right] \quad (23)$$

The proportional gain, can be estimated using:

$$K_P = K\tau_Z = K_I\tau_Z = K_I\frac{\tau'_L}{n} = K_I\frac{R_t}{\beta R_E}\frac{\tau_L}{n} \quad (24)$$

III. RESULTS

The solutions described in section II, where simulated using controllers with different parameters.

Based on the characteristics of the available magnet, all simulations were performed considering the following values for the flux density:

- B_{MI} =0.2 T;
- B_{M0} =0.05 T.

Considering a typical cycle of a FFC NMR experiment, the time intervals used are:

- Δt_{MI}=0.197 s;
- Δt_{M0}=0.297 s;
- Δt_r=3x10^{-3} s;
- Δf=3x10^{-3} s.

In order to compare the performance of the two controllers, the proposed system was simulated considering step and ramp inputs. Furthermore, simulation results with different tuning parameters are shown in order to note the dynamics observed.

A. Simulations using the PD2I controller

The PD2I controller is simulated using two different sets of parameters (Table I) and imposing step and ramp inputs.

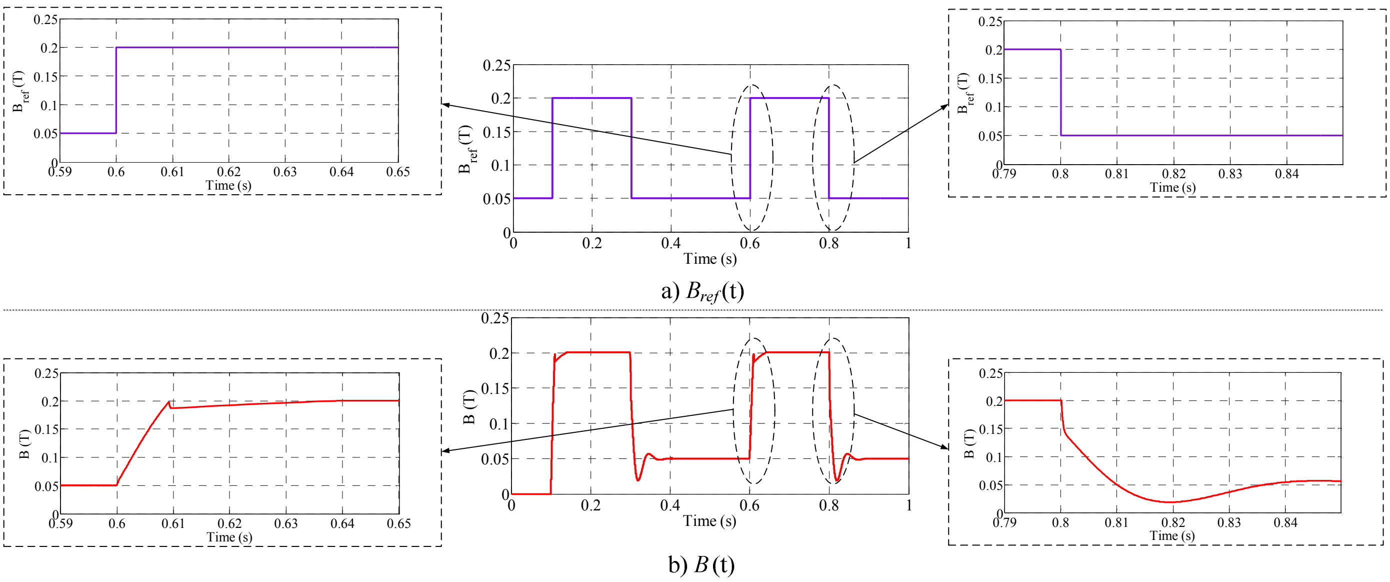

Fig. 6. Simulations using a PD2I controller for a step input and the set #1 of parameters.

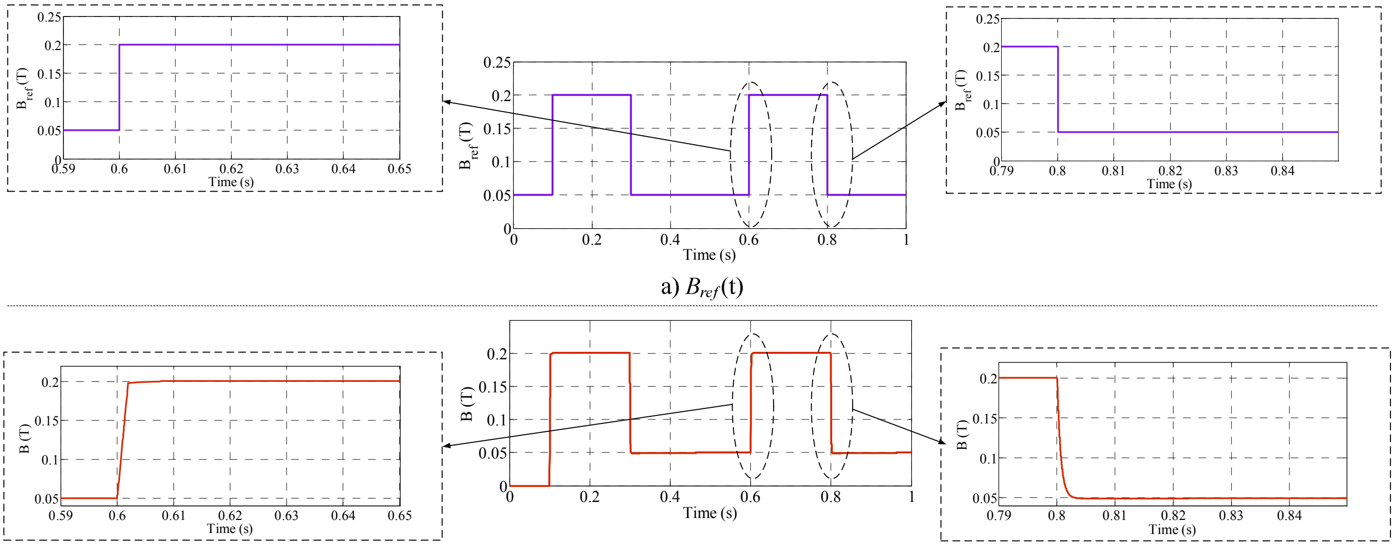

a) $B_{ref}(t)$

b) $B(t)$

Fig. 7. Simulations using a PD2I controller for a step input and the set #2 of parameters.

TABLE I. PD2I CONTROLLER PARAMETERS

	Set #1	Set #2
K_P	6.37	80
K_D	0.05	0.05
K_{I1}	1000	1000
K_{I2}	100	5000

The simulations results obtained for the PD2I controller imposing a step input, considering the two parameters sets, are shown in Fig. 6 and Fig. 7.

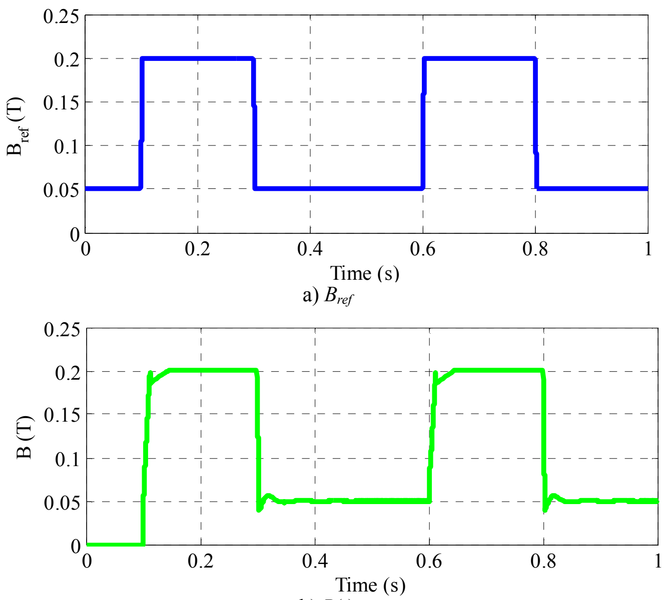

a) B_{ref}

b) $B(t)$

Fig. 8. Simulations using a PD2I controller for a ramp input (set #1 of parameters).

In Fig. 8 and Fig. 9 are presented the simulations results for the PD2I controller for a ramp input.

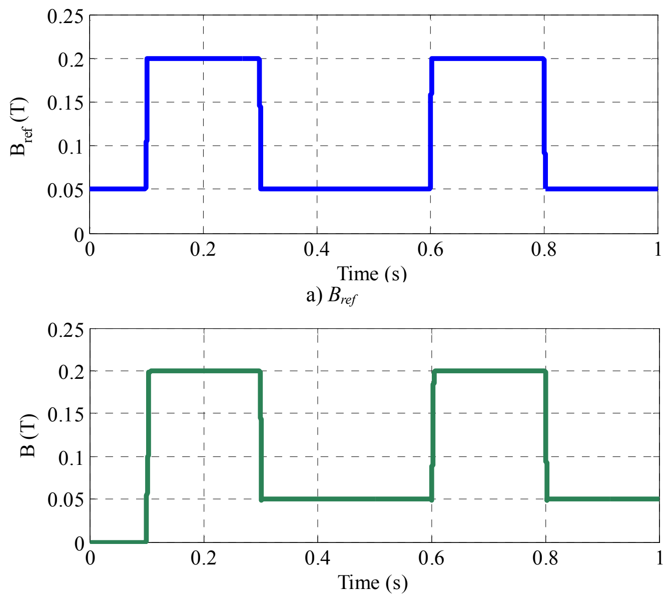

a) B_{ref}

b) $B(t)$

Fig. 9. Simulations using a PD2I controller for a ramp input (set #2 of parameters).

B. Simulations using the PI controller

In the figures below, simulations performed imposing a step input and a ramp input, respectively, are performed using the following two sets of parameters for a PI controller:

- K_P=500;
- K_I=50000.

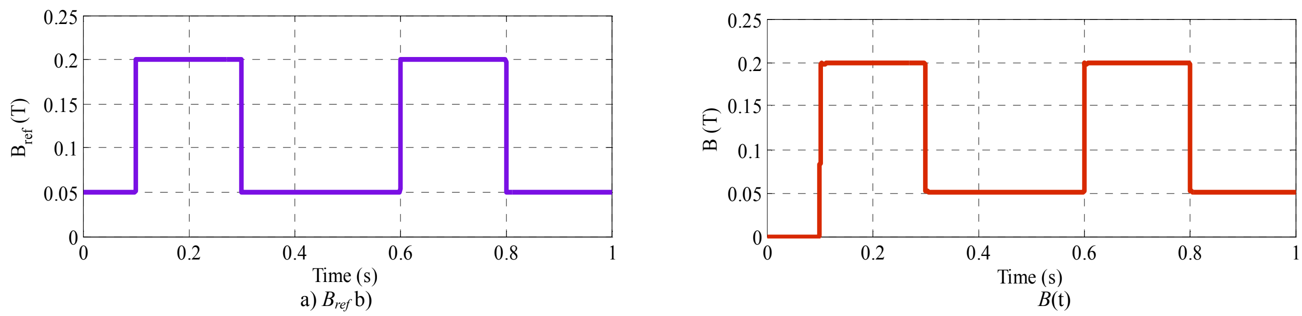

Fig. 10. Simulations using a PI controller for a step input.

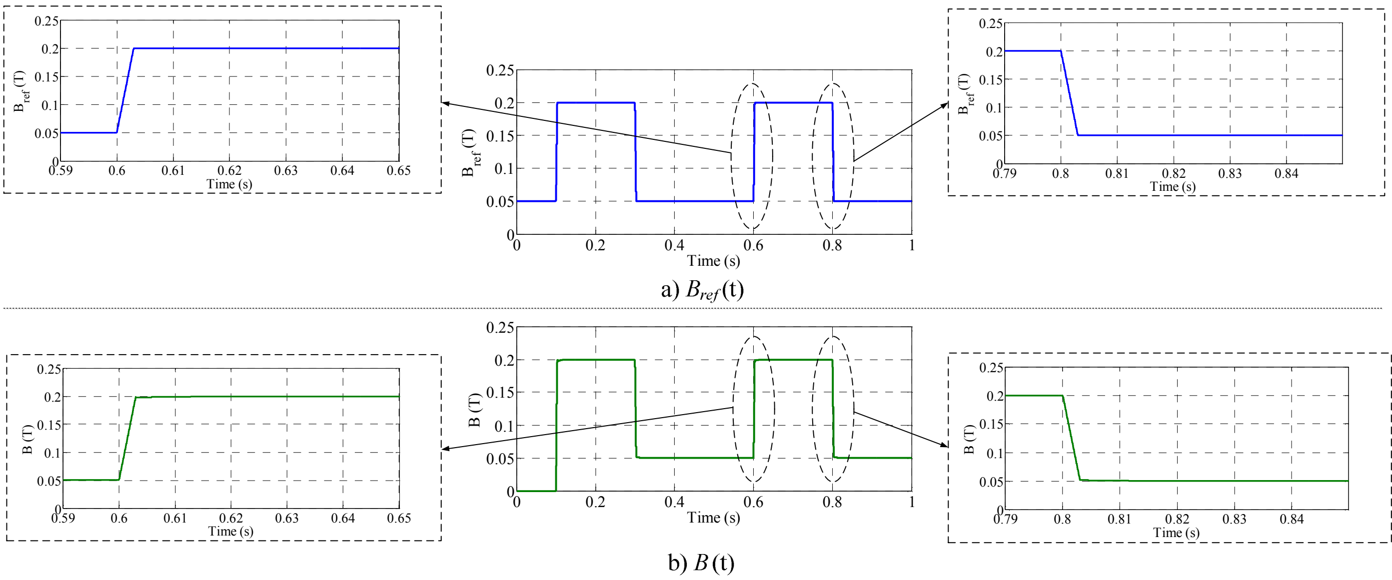

Fig. 11. Simulations using a PI controller for a ramp input.

As it can be observed in the previous figures, both controllers fulfill the requirements of the application. Anyway, considering that fast transients are required, the dynamics observed when imposing step inputs are adequate. Furthermore, the easier tuning and less complexity of the PI controller are factors that should be balanced. So that, in the developed prototype [10, 14], a PI controller was implemented successfully.

C. *Experimental results using the PI controller*

In Fig. 12 and Fig. 13, experimental results for the flux density using a PI controller are shown.

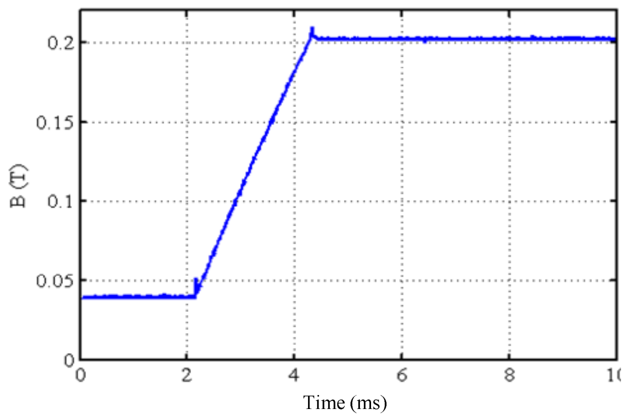

Fig. 12. Experimental "Up" transient using a PI controller for a step input.

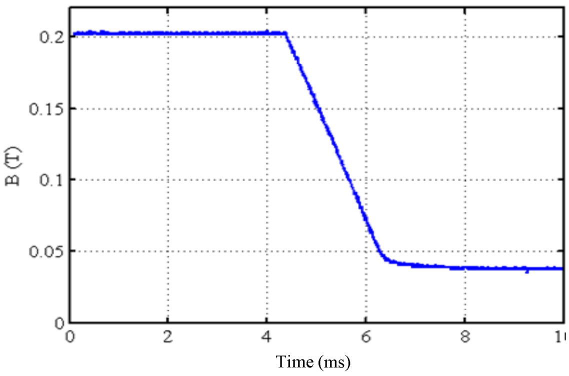

Fig. 13. Experimental “Down” transient using a PI controller for a step input.

As it can be observed, the experimental results fulfil the requirements of the application, i.e., fast transients without oscillations.

IV. Conclusion

In this paper, simulations results of a FFC NMR power supply controlled using two controllers with different configurations are shown. Both controllers fulfil the requirements of the application, but the option was taken choosing the controller with less complexity and easier to tune since it can be implemented analogically or digitally.

Acknowledgment

This work was supported by national funds through *FCT – Fundação para a Ciência e a Tecnologia*, under project PEst-OE/EEI/LA0021/2013.

References

[1] F. Noack, “NMR Field-Cycling Spectroscopy: Principles and Applications”, *Prog. NMR Spectrosc*., vol. 18, pp. 171-276, 1986.

[2] R. Seitter, R. O. Kimmich, “Magnetic Resonance: Relaxometers”, *Encyclopedia of Spectroscopy and Spectrometry*, Academic Press, London, pp. 2000-2008, 1999.

[3] E. Anoardo, G. Galli, G. Ferrante, “Fast-Field-Cycling NMR: Applications and Instrumentation”, *Applied Magnetic Resonance*, vol. 20, pp. 365-404, 2001.

[4] R. Kimmich and E. Anoardo, “Field-Cycling NMR relaxometry”, *Progress in NMR Spectroscopy*, 44, pp. 257-320, 2004.

[5] J. Constantin, J. Zajicek, F. Brown, “Fast Field-Cycling Nuclear Magnetic Resonance Spectrometer”, *Rev. Sci. Instrum.*, vol. 67, pp. 2113-2122, 1996.

[6] D. M. Sousa, P. A. L. Fernandes, G. D. Marques, A. C. Ribeiro, P. J. Sebastião, “Novel Pulsed Switched Power Supply for a Fast Field Cycling NMR Spectrometer”, *Solid State Nuclear Magnetic Resonance*, vol. 25, pp. 160-166, 2004.

[7] D. M. Sousa, G. D. Marques, J. M. Cascais, P. J. Sebastião, “Desktop Fast-Field Cycling Nuclear Magnetic Resonance Relaxometer”, *Solid State Nuclear Magnetic Resonance*, vol. 38, pp. 36-43, 2010.

[8] A. Roque, S. F. Pinto, J. Santana, Duarte M. Sousa, E. Margato, J. Maia, “Dynamic Behavior of Two Power Supplies for FFC NMR Relaxometers”, IEEE International Conference on Industrial Technology – ICIT 2012, Athens - Greece, 2012.

[9] D. M. Sousa, E. Rommel, J. Santana, J. Fernando Silva, P. J. Sebastião, A. C. Ribeiro, “Power Supply for a Fast Field Cycling NMR Spectrometer Using IGBTs Operating in the Active Zone”, 7th European Conference on POWER ELECTRONICS AND APPLICATIONS, , Trondheim, Norway, pp. 2.285-2.290, 1997.

[10] A. Roque, D. M. Sousa, E. Margato, J. Maia and Gil Marques, “Control and Dynamic Behaviour of a FFC NMR Power Supply - Power Consumption and Power Losses”, IECON 2013 – 39th Annual Conference of the IEEE Industrial Electronics Society, Vienna, Austria, 2013.

[11] K. Ogata, “Modern Control Engineering”, 5th Edition, Prentice-Hall, 2010.

[12] A. G. Redfield, W. Fite, H. E. Bleich, “Precision High Speed Current Regulators for Occasionally Switched Inductive Loads”, *Review of Scientific Instruments*, vol. 39, pp. 710-715, 1968.

[13] J. J. D'Azzo and C. H. Houpis, “Linear Control System Analysis and Design: Conventional and Modern”, 4th Edition, McGraw-Hill, 1995.

[14] D. M. Sousa, G. Marques and P. J. Sebastião, “Reducing the size of Fast Field Cycling NMR Spectrometers based on the use of IGBTs”, “IEEE ICIT 2009 - International Conference on Industrial Technology”, Churchill - Australia, February 2009.